Neuropsychopharmacology

ARTICLE

Isoform-selective phosphoinositide 3-kinase inhibition ameliorates a broad range of fragile X syndrome-associated deficits in a mouse model

Christina Gross[1,2], Anwesha Banerjee[3], Durgesh Tiwari[1], Francesco Longo[4], Angela R. White[1], A. G. Allen[5,6], Lindsay M. Schroeder-Carter[1], Joseph C. Krzeski[1], Nada A. Elsayed[1], Rosemary Puckett[4], Eric Klann[4], Ralph A. Rivero[7], Shannon L. Gourley[5,6,8] and Gary J. Bassell[3,9]

Defects in the phosphoinositide 3-kinase (PI3K) pathway are shared characteristics in several brain disorders, including the inherited intellectual disability and autism spectrum disorder, fragile X syndrome (FXS). PI3K signaling therefore could serve as a therapeutic target for FXS and other brain disorders. However, broad inhibition of such a central signal transduction pathway involved in essential cellular functions may produce deleterious side effects. Pharmacological strategies that selectively correct the overactive components of the PI3K pathway while leaving other parts of the pathway intact may overcome these challenges. Here, we provide the first evidence that disease mechanism-based PI3K isoform-specific inhibition may be a viable treatment option for FXS. FXS is caused by loss of the fragile X mental retardation protein (FMRP), which translationally represses specific messenger RNAs, including the PI3K catalytic isoform p110β. FMRP deficiency increases p110β protein levels and activity in FXS mouse models and in cells from subjects with FXS. Here, we show that a novel, brain-permeable p110β-specific inhibitor, GSK2702926A, ameliorates FXS-associated phenotypes on molecular, cellular, behavioral, and cognitive levels in two different FMRP-deficient mouse models. Rescued phenotypes included increased PI3K downstream signaling, protein synthesis rates, and dendritic spine density, as well as impaired social interaction and higher-order cognition. Several p110β-selective inhibitors, for example, a molecule from the same chemotype as GSK2702926A, are currently being evaluated in clinical trials to treat cancer. Our results suggest that repurposing p110β inhibitors to treat cognitive and behavioral defects may be a promising disease-modifying strategy for FXS and other brain disorders.

Neuropsychopharmacology (2019) 44:324–333; https://doi.org/10.1038/s41386-018-0150-5

INTRODUCTION

Signaling through the phosphoinositide 3-kinase (PI3K)/mechanistic target of rapamycin (mTOR) pathway is altered in several brain disorders, suggesting shared underlying disease mechanisms and potential therapeutic targets [1, 2]. One prominent example of a mental disorder that has been associated with defects in the PI3K/mTOR pathway is fragile X syndrome (FXS) [3]. FXS is an inherited intellectual disability and often associated with autism. In most cases, it is caused by the transcriptional silencing of the fragile X mental retardation gene 1 (*FMR1*), which leads to loss of the fragile X mental retardation protein (FMRP) [4]. FMRP is a messenger RNA (mRNA)-binding protein that regulates the translation of specific mRNAs. In the absence of FMRP, general protein synthesis, as well as the translation of many of its target mRNAs, are dysregulated [5–7], but it is unclear which of these proteins or mechanisms are the most suitable and effective targets for therapeutic interventions. In the initial studies revealing molecular and cellular dysfunctions in FXS, signaling through the metabotropic glutamate receptors 1 and 5 (mGlu1/5) was found to be exaggerated [8], and thus suggested as therapeutic target [9]. So far, clinical trials using mGlu1/5 antagonists have not shown the expected results [10, 11], which has initiated efforts to identify and test other treatment strategies

Apart from mGlu1/5, many additional neurotransmitter receptor pathways are affected in FXS, including Gq-coupled, TrkB, or dopamine receptors [3]. These findings hint towards a defect within common downstream signaling molecules, and indeed, PI3K, extracellular signal-regulated kinases 1/2, and mTOR/S6K1 signaling are altered in FXS mouse models and patient cells [3, 4]. The PI3K complex is of special interest, because several components of this signaling pathway have been identified and confirmed as mRNA targets of FMRP, for example, the PI3K catalytic isoform p110β [14–19]. We have recently shown that genetic reduction of p110β rescues molecular, cellular, behavioral, and cognitive deficits in FXS mouse models [20]. Genetic rescue provides motivation to

[1]Division of Neurology, Cincinnati Children's Hospital Medical Center, Cincinnati, OH 45229, USA; [2]Department of Pediatrics, College of Medicine, University of Cincinnati, Cincinnati, OH 45229, USA; [3]Department of Cell Biology, Emory University School of Medicine, Atlanta, GA 30322, USA; [4]Center for Neural Science, New York University, New York, NY 10003, USA; [5]Department of Pediatrics, Emory University School of Medicine, Atlanta, GA 30322, USA; [6]Department of Psychiatry and Behavioral Sciences, Emory University School of Medicine, Atlanta, GA 30322, USA; [7]GlaxoSmithKline, Collegeville, PA 19426, USA and [8]Yerkes National Primate Research Center, Emory University School of Medicine, Atlanta, GA 30329, USA and [9]Present address: Department of Neurology, Emory University School of Medicine, Atlanta, GA 30322, USA
Correspondence: Christina Gross (christina.gross@cchmc.org) or Shannon L. Gourley (shannon.l.gourley@emory.edu) or Gary J. Bassell (gary.bassell@emory.edu)

Received: 26 January 2018 Revised: 7 June 2018 Accepted: 1 July 2018
Published online: 13 July 2018

consider pharmacologic strategies. P110β-selective inhibitors reduce tumor growth in animal models and are currently being evaluated for the use in humans with cancer [21, 22]. However, the efficacy of p110β inhibitors in animal models of mental disorders has not been tested before. Here, we show that a novel potent central nervous system (CNS)-penetrant PI3K antagonist (GSK2702926A (GSK6A)) from the same chemotype as a compound that is currently tested in clinical trials for cancer and with high selectivity for the catalytic isoform p110β, rescues phenotypes on molecular, cellular, behavioral, and cognitive levels in *Fmr1* knockout (*Fmr1*^{KO}) and knockdown mice. Our results suggest that PI3K isoform-selective inhibitors developed for cancer treatment could be considered for repurposing as a disease mechanism-targeted treatment in FXS.

MATERIALS AND METHODS

Animals

Fmr1^{KO} mice maintained on a C57BL/6 background and C57BL/6 wild-type (WT) mice were obtained from The Jackson Laboratory (Bar Harbor, ME, USA). Sprague–Dawley rats and Crl:CD-1-Foxn1 mice for pharmacokinetic studies were obtained from Charles River Laboratories (Burlington, MA, USA). The animal protocol was approved by the Institutional Animal Care and Use Committees of Emory University, NYU, CCHMC, and GlaxoSmithKline, and complied with the Guide for the Care and Use of Laboratory Animals. For details on breeding schemes and age of experimental mice see Supplementary Materials and Methods.

Drugs, antibodies, and lentiviral vectors

GSK6A was synthesized at GlaxoSmithKline (for details see ref. [23]) and injected intraperitoneally at a dose of 5 mg/kg (0.01 g/ml in 10% dimethyl sulfoxide (DMSO) (BioWorld, Dublin, OH)). Vehicle control was 10% DMSO. A description of antibodies and viral vectors is provided in Supplementary Materials and Methods.

SDS-PAGE and western blotting

Sodium dodecyl sulfate-polyacrylamide gel electrophoresis (SDS-PAGE) and Western blotting were performed as described previously [20]. Where applicable, tissue was collected for 1.5 h (Fig. 1c, d; Figs. S2a–d, S3a–f) or 1 h (Fig. 5d; Figs. S2g–i, S3g–j) or 1 and 24 h (Fig. S2e, f; as indicated) after drug injection. Equal amounts of protein were loaded in duplicates. Molecular weight standards were run on every gel, and signals were detected by autoradiography. Contrast of scanned western blots was enhanced using Photoshop CS6 (Adobe Systems, San Jose, CA, USA). Details on brain tissue dissection are provided in Supplementary Materials and Methods.

Protein synthesis assay

Four hundred-micrometer-thick hippocampal slices from 3- to 6-week-old *Fmr1*^{KO} mice and WT littermates were prepared as described [24] and submerged in oxygenated artificial cerebrospinal fluid (ACSF) treated with vehicle or 1 μM GSK6A. After 30 min, 1 μg/ml puromycin (Invitrogen, Carlsbad, CA, USA) was added. Forty-five minutes later, slices were flash frozen on dry ice and stored at −80 °C. For analysis, slices were lysed using sonication [18]. Equal amounts of protein were loaded on a SDS-PAGE and analyzed by puromycin-specific western blotting and densitometry using ImageJ (NIH, Bethesda, MD, USA). Signal from hippocampal slices without puromycin treatment was subtracted as background.

Dendritic spine analysis

Dendritic spines of pyramidal neurons in the hippocampal CA1 area (bregma levels −1.8 to −2.2) were analyzed in 65–70-day-old mice that had received daily injections of GSK6A or vehicle for 10 days using the FD Rapid GolgiStain Kit from FD Neurotechnologies, Inc. (Columbia, MD, USA) as described previously [20]. Brains were harvested 1 h after the last injection. After Golgi impregnation, 160-μm-thick slices were stained according to the manufacturer's guidelines and imaged using a Nikon inverted microscope with a 60x oil objective. Dendritic spine numbers were counted using ImageJ. Analyzed dendritic segments from secondary apical dendrites were between 50 and 150 μm in length, and at least 100 μm distant from the soma. We analyzed 4–5 brains per condition, 5–7 neurons per brain, and 1–2 dendrites per neuron.

Hippocampal mGluR-LTD

(*S*)-3,5-dihydroxyphenylglycine (DHPG)-induced metabotropic glutamate receptor-long-term depression (mGluR-LTD) on hippocampal slices from 3- to 6-week-old WT or *Fmr1*^{KO} mice was performed as described previously [24]. Mice were injected with GSK6A or vehicle and euthanized after 1 h. Four hundred micrometer-thick hippocampal slices were incubated in oxygenated ACSF for 45 min, followed by bath application of 1 μM GSK6A or vehicle for 15 min, baseline recording for 30 min, and 50 μM DHPG application for 10 min. Fifty minutes after DHPG, GSK6A or vehicle were washed out and recordings continued for another 40 min. For details see Supplementary Materials and Methods.

Nesting behavior

Nest construction was assessed 24 h after a new nestlet was placed in the home cage as described [20, 25]. All mice received drug or vehicle injections when the nestlet was placed in the cage. One group of mice additionally received one drug or vehicle injection 24 h before the start of the assay.

Marble burying

Marble burying was assessed as described [20] using 20 dark blue glass marbles arranged in a grid on 10 cm bedding in large cages 1 h after injection. For details see Supplementary Materials and Methods.

Audiogenic seizures

Mice were tested at postnatal days 18–22, in groups of two between 6:30 and 8:00 p.m. as described previously [20, 26]. One group of mice received injections 1 h before testing (Fig. 2d; Fig. S4c). A separate group received two injections, 24 and 1 h before testing (Fig. 2e; Fig. S4d, e). Mice were euthanized 30 min after the procedure; cortex and hippocampus were dissected and flash frozen on dry ice.

Open field activity

Open field activity was analyzed 1 h after injection as described previously [27]. For details see Supplementary Materials and Methods.

Three-chamber social interaction assay

Social behavior was measured using the three-chamber social interaction assay as described previously [28]. The mice received injections 1 h before testing. For details see Supplementary Materials and Methods.

Self-grooming

Mice were scored for spontaneous grooming behaviors. Each mouse was placed individually into a standard mouse cage, illuminated at ~100 lx. Trials were video-recorded for 10 min, and time spent grooming was recorded by a blinded rater. Mice received injections 1 h prior to the test.

Generation of prefrontal cortex-selective *Fmr1* knockdown mice and behavioral testing of complex decision making

Prefrontal cortex-selective *Fmr1* knockdown mice were generated and higher-order decision-making strategies were tested as

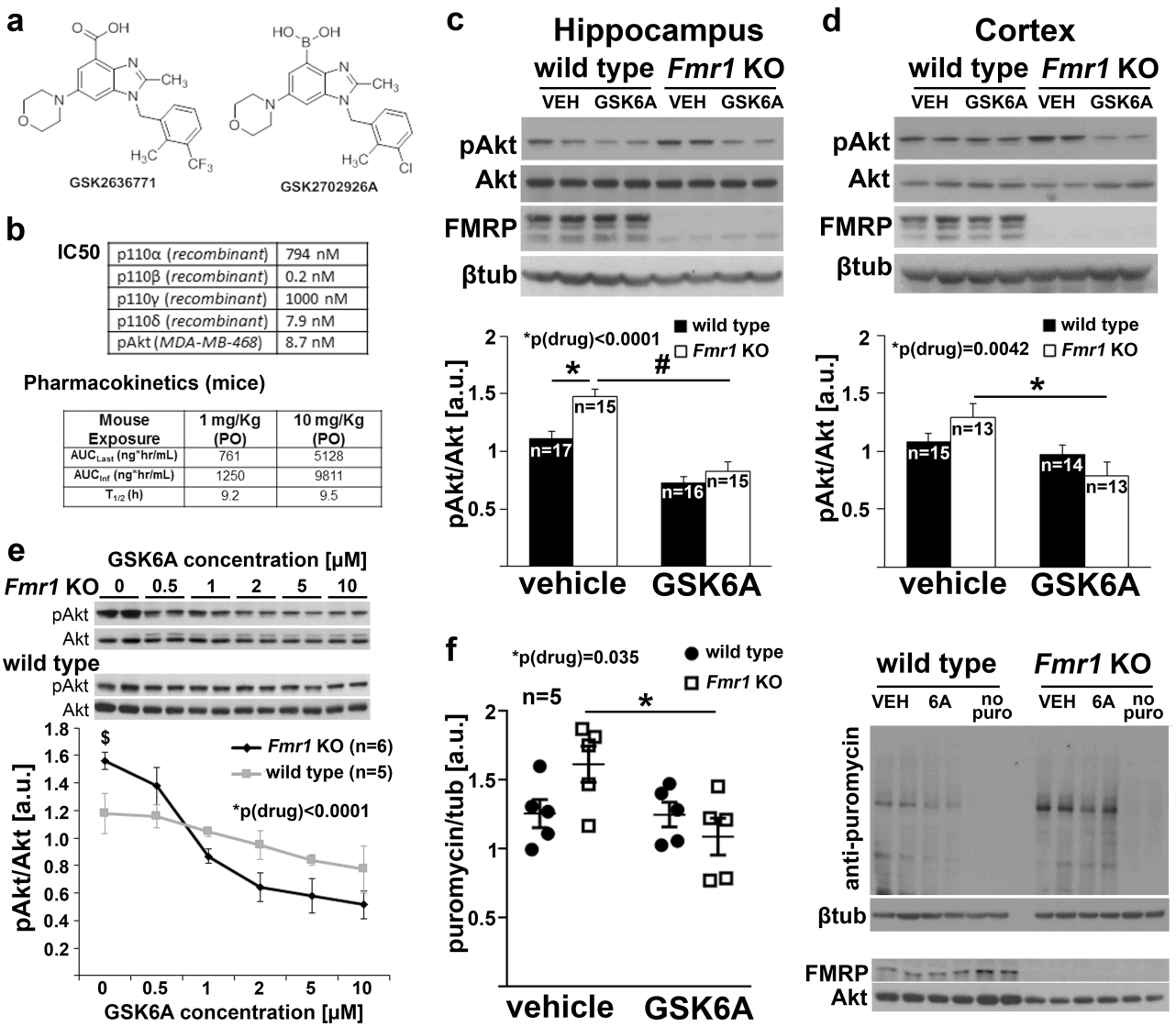

Fig. 1 The p110β-selective inhibitor GSK2702926A reduces elevated protein synthesis and Akt phosphorylation in *Fmr1*^{KO} mice. **a**, **b** Structures of GSK2636771 and GSK2702926A (**a**), and drug metabolism and pharmacokinetic properties of GSK2702926A (**b**), a highly selective and potent p110β antagonist. See Fig. S1 and Supplementary Materials and Methods for further details. **c**, **d** Intraperitoneal injection of 5 mg/kg GSK6A significantly reduces Akt phosphorylation at threonine 308 1.5 h after injection in hippocampal (**c**: two-way ANOVA with Tukey's post hoc tests: p(drug) <0.0001, F(1,59) = 55.4; p(genotype) = 0.0015, F(1,59) = 11.0; p(interaction) = 0.059, F(1,59) = 3.7; $^{*}p = 0.002$, $^{\#}p < 0.0001$) and cortical lysates (**d**: two-way ANOVA with Tukey's post hoc tests: p(drug) = 0.0042, F(1,51) = 9.0; p(genotype) = 0.902, F(1,51) = 0.02; p(interaction) = 0.059, F(1,51) = 3.7; p(wt/veh-ko/veh) = 0.47, $^{*}p = 0.007$). Phospho-Akt-specific signals were normalized to Akt; representative western blots are shown on top. Akt levels did not differ between groups (Fig. S2c, d). **e** A dose–response curve assessing the effect of a 30 min bath application of GSK6A on Akt phosphorylation in hippocampal slices from naïve WT and *Fmr1*^{KO} mice indicates that p110β-selective inhibition has a significantly stronger effect on Akt phosphorylation in *Fmr1*^{KO} hippocampus compared to WT (two-way ANOVA with repeated measures with Tukey's post hoc tests: p(drug) < 0.0001, F(5,45) = 14.1; p(genotype) = 0.054, F(1,9) = 4.9; p(interaction) = 0.012, F(5,45) = 3.3; $^{\$}p = 0.079$). Phospho-Akt was normalized to Akt; representative western blots are shown on top. Further analysis of drug and genotype effects on Akt and S6 phosphorylation are shown in Figs. S2 and S3. **f** Treatment of hippocampal brain slices with 1 μM GSK6A for 30 min significantly reduced protein synthesis rates in *Fmr1*^{KO}, but not WT mice (two-way ANOVA with Tukey's post hoc tests: p(drug) = 0.035, F(1,16) = 5.3; p(genotype) = 0.404, F(1,16) = 0.7; p(interaction) = 0.041, F(1,16) = 5.0; p(wt/veh-ko/veh) = 0.27, $^{*}p = 0.033$). Puromycin-specific signal was normalized to β-tubulin and "no puromycin" background signal was subtracted. Representative western blots are shown at right and in Fig. S4a. FMRP-specific blots in **c**, **d**, and **f** (run on separate gels) confirm the genotype

described [20]. Drug or vehicle were injected three times: after response-outcome contingency training, after reversal training and after the first day of extinction. For details, see Supplementary Materials and Methods.

Statistical analyses

Statistical analyses were performed using GraphPad Prism, SigmaStat, and SPSS. Statistical tests were chosen based on study design (indicated in the figure legends). Tukey's post hoc analyses between WT and *Fmr1*^{KO} vehicle treated, as well as WT vehicle and *Fmr1*^{KO} GSK6A treated were performed for two-way analysis of variance (ANOVA) with significant interaction or main effects ($p \le 0.05$). All statistics are reported in the figure and/or legends. Sample sizes were based on previous studies [20, 24]. Outliers were defined as animals that differed more than 2 × standard deviation from the mean and are indicated in Supplementary Materials and Methods.

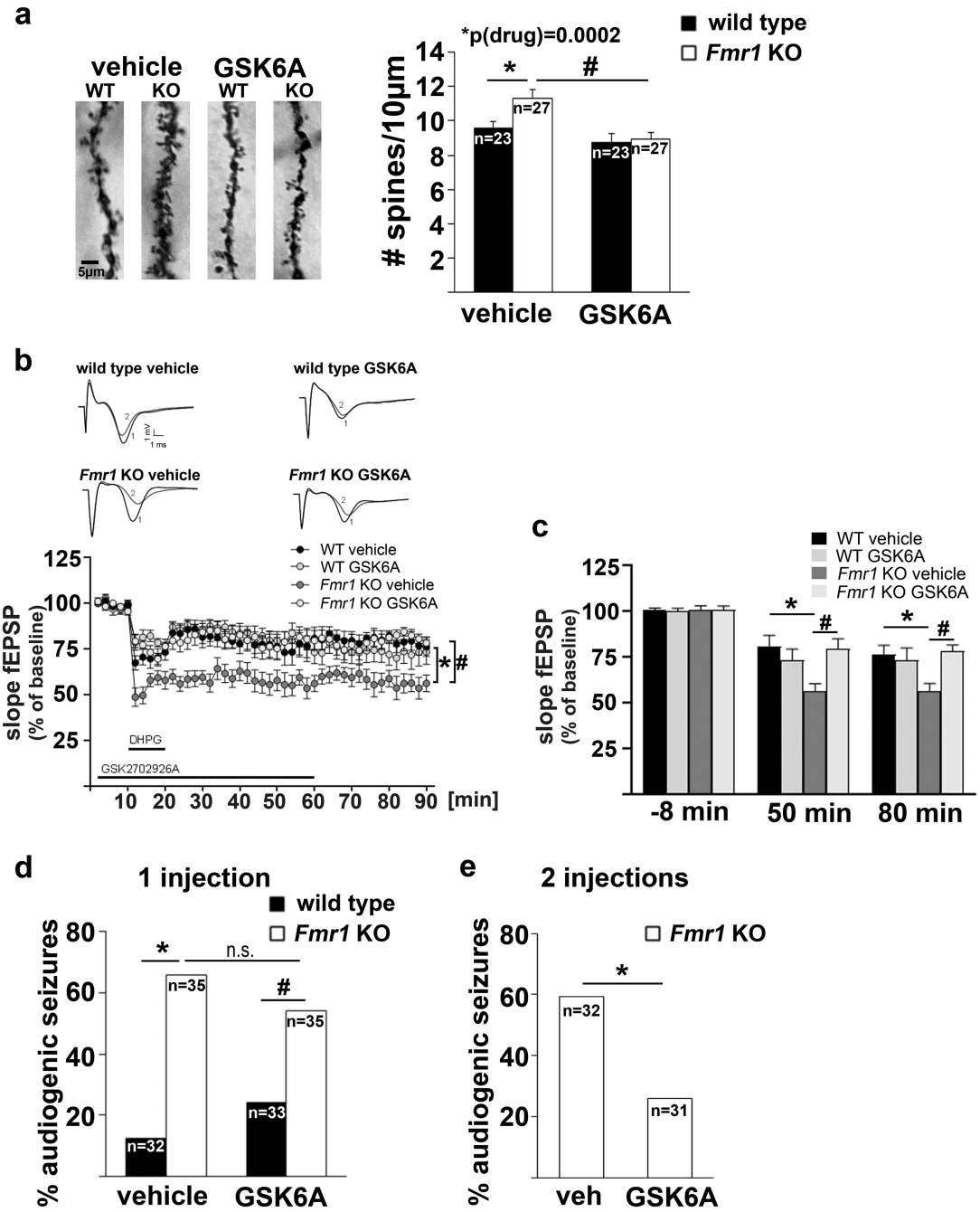

Fig. 2 Pharmacological inhibition of p110β normalizes increased dendritic spine density, synaptic plasticity, and neuronal excitability in *Fmr1*^{KO} mice. **a** Ten daily injections of 5 mg/kg GSK6A significantly reduced dendritic spine density on apical secondary dendrites from pyramidal CA1 neurons in the hippocampus of *Fmr1*^{KO} and WT mice (two-way ANOVA with Tukey's post hoc tests: p(drug) = 0.0002, F(1,96) = 14.9; p(genotype) = 0.026, F(1,96) = 5.1; p(interaction) = 0.066, F(1,96) = 3.5; $^{*}p = 0.023$, $^{\#}p = 0.003$). Representative dendrites are shown at left. **b**, **c** GSK6A normalizes exaggerated mGlu1/5-dependent LTD in *Fmr1*^{KO} hippocampal slices. Mice were i.p. injected with either 5 mg/kg GSK6A or vehicle 1 h before preparation of hippocampal slices. GSK6A (1 µM) and DHPG (50 µM) incubation periods are indicated in the figure. **b** Mean baseline-normalized field excitatory postsynaptic potentials (fEPSPs) are represented as a function of time (WT vehicle: $n = 16$; WT drug: $n = 13$; *Fmr1*^{KO} vehicle: $n = 13$; *Fmr1*^{KO} drug: $n = 12$; two-way ANOVA (condition × time) with repeated measures: p(interaction) = 0.006, F(117,1404) = 1.375; Tukey's post hoc tests: $^{*}p < 0.0001$, $^{\#}p = 0.002$). Representative traces are shown on top (1, black = baseline; 2, gray = after LTD). **c** Mean fEPSPs at 8 min before, and 50 and 80 min after DHPG (two-way ANOVA (condition × time), p(time) < 0.0001, F(2,146) = 54.13; p(condition) = 0.0001, F(3,146) = 7.3; p(interaction) = 0.075, F(6,146) = 2.0); Tukey's post hoc tests: $^{*}p(50) = 0.0006$; $^{\#}p(50) = 0.0026$; $^{*}p(80) = 0.008$; $^{\#}p(80) = 0.007$). GSK6A reduced induction of LTD in both WT and *Fmr1* KO mice (Fig. S4b). **d** One hour after a single injection of GSK6A, no significant difference in audiogenic seizure susceptibility compared to vehicle treatment was detected in *Fmr1*^{KO} (Fisher's exact test, $p = 0.464$) or WT mice (Fisher's exact test, $p = 0.339$), and audiogenic seizure susceptibility was still significantly higher in *Fmr1*^{KO} mice than WT mice (Fisher's exact tests, $^{*}p < 0.0001$, $^{\#}p = 0.014$). **e** Two consecutive GSK6A injections 24 h apart significantly reduced audiogenic seizure susceptibility in *Fmr1*^{KO} mice (Fisher's exact test, $^{*}p = 0.011$). Similar results were observed using a seizure scoring system (Fig. S4c, d). Experiments were performed using male mice, except of **e**, for which male and female mice were used. No differences in seizure susceptibility or drug effect were observed in male compared to female mice (Fig. S4e)

RESULTS

A novel brain-permeable p110β-selective inhibitor normalizes increased Akt phosphorylation and protein synthesis in *Fmr1*^{KO} mice

This study tests a novel potent CNS-permeable p110β-selective inhibitor developed by GlaxoSmithKline ("GSK6A" hereafter) for its capability to rescue molecular, cellular, behavioral, and cognitive defects in mouse models of FXS. GSK6A is based on a series of p110β-selective inhibitors that were recently developed [23, 29]. It maintains the key pharmacophoric elements found in the clinical compound (GSK2636771), which is currently in phase II development for treatment of PTEN-loss advanced solid tumors in adults (Fig. 1a). In contrast to the clinical compound, GSK6A is CNS-permeable and, thus, suitable to modulate brain function. GSK6A is potent and selective for p110β and shows good oral bioavailability and high drug exposure in mice (Fig. 1b). The brain/blood ratio is 1.32 in rats (Fig. S1), suggesting good brain permeability in mice as well [30]. Indeed, intraperitoneal (i.p.) injection of GSK6A in vivo significantly reduced Akt phosphorylation in hippocampal and cortical lysates of WT and *Fmr1*^{KO} mice 1.5 h later, confirming that the drug crosses the blood–brain barrier efficiently in mice (Fig. 1c, d). The mice were subject to a sound stimulation to test for audiogenic seizure susceptibility (see Fig. 2d, e) 30 min before tissue extraction, but seizures did not affect Akt phosphorylation, and GSK6A reduced Akt phosphorylation in seized and non-seized *Fmr1*^{KO} mice (Fig. S2a, b; timeline shown in Fig. S5d). Moreover, reduced Akt phosphorylation 1 h after GSK6A injection was confirmed in another cohort of naïve *Fmr1*^{KO} mice that had not experienced a sound stimulation, and the drug effect was not detectable anymore 24 h after drug injection (Fig. S2e, f).

Extensive brain region-specific analyses in a different cohort of naïve mice further suggested that the effect of the drug to reduce Akt phosphorylation in *Fmr1*^{KO} mice is widespread throughout the brain, including amygdala, paraventricular nucleus of the thalamus, and nucleus accumbens (Fig. S2g–i). In WT mice, a significant drug effect on Akt phosphorylation was only detected in hippocampal lysates but not the cortex. This may be due to higher expression levels of p110β in WT cortex compared to hippocampus, as observed in humans [31], possibly requiring higher doses of the p110β inhibitor to be effective in cortex.

We next assessed the effect of drug and genotype on phosphorylation of S6, a downstream target of PI3K/mTOR previously shown to be increased in *Fmr1*^{KO} mice [24]. We tested both sound-exposed (Fig. S3a–f) and naïve mice (Fig. S3g–j), and quantified phosphorylation at two different sites, namely Ser235/236 (Fig. S3a–d, g, h), which is regulated by multiple signaling pathways [32], and at Ser240/244 (Fig. S3e–j), which is predominantly phosphorylated through the PI3K-mTOR-S6K1 pathway [33]. In contrast to Akt, S6 phosphorylation was not significantly affected by genotype or drug, except of Ser240/244 phosphorylation in the cortex, where a drug effect, but no differences in pairwise comparisons, was detected (Fig. S3j).

A dose–response analysis in vitro showed that Akt phosphorylation was reduced 30 min after drug exposure with increasing concentrations of GSK6A in hippocampal slices of WT and *Fmr1*^{KO} mice, and that Akt phosphorylation in *Fmr1*^{KO} slices was affected more strongly (Fig. 1e). To assess how GSK6A influences protein synthesis rates in FXS mice, we measured incorporation of puromycin into nascent peptide chains in hippocampal slices through western blot quantification [24, 34]. Treatment of hippocampal slices with 1 µM GSK6A for 30 min significantly reduced protein synthesis rates in *Fmr1*^{KO} hippocampal slices, but did not significantly affect WT slices (Fig. 1f; Fig. S4a), consistent with the hypothesis that excess PI3K activity contributes to elevated protein synthesis in FXS.

P110β-selective inhibition reduces aberrantly increased dendritic spine density and mGlu1/5-LTD in *Fmr1*^{KO} mice

Increased dendritic spine density in the hippocampus and cortex is a well-characterized phenotype in humans with FXS and in *Fmr1*^{KO} mice [3]. Based on the assumption that changes in dendritic spine density require a longer drug exposure time than modifying protein phosphorylation, as well as our results that the drug effect was undetectable after 24 h, we anticipated that chronic treatment with the drug was needed to normalize dendritic spine density in *Fmr1*^{KO} mice. We used Golgi-Cox staining of hippocampal neurons to show that daily administration of GSK6A over 10 days reduced dendritic spine density on secondary apical dendrites of CA1 pyramidal neurons in both WT and *Fmr1*^{KO} mice (Fig. 2a).

Fmr1^{KO} mice show exaggerated hippocampal mGlu1/5-dependent LTD [8]. To determine whether GSK6A normalizes LTD, mice were injected with either GSK6A or vehicle 1 h before hippocampal slice preparation. To avoid drug washout during LTD measurement, hippocampal slices were kept in either 1 µM GSK6A or vehicle during baseline recordings, during DHPG treatment, and for 50 min after induction of LTD. GSK6A treatment normalized mGlu1/5-LTD in *Fmr1*^{KO} mice at 50 and 80 min after LTD induction (Fig. 2b, c). This effect was sustained after drug removal. In both WT and *Fmr1*^{KO} mice, GSK6A reduced induction of LTD immediately after DHPG application (Fig. S4b), as was previously observed in *Fmr1*^{KO} mice with genetic deletion of S6K1 [24]. We thus cannot exclude the possibility that the observed rescue of LTD in *Fmr1*^{KO} mice after GSK6A treatment was caused by a genotype-independent reduction in the induction of LTD.

GSK6A reduces susceptibility to audiogenic seizures in *Fmr1*^{KO} mice

Fmr1^{KO} mice have increased susceptibility to sound-induced (audiogenic) seizures [35]. One injection of GSK6A 1 h before testing did not significantly change audiogenic seizure susceptibility in male *Fmr1*^{KO} or WT mice (Fig. 2d), despite of reduced Akt phosphorylation throughout the brain (Fig. 1c, d; Fig. S2). Similar trends were observed when using a scoring scale that takes into account wild running and death (Fig. S4c). GSK6A seemed to increase seizure susceptibility in WT mice after one dose (12.5% vs. 24.24%), but the effect was not significant ($p = 0.34$). The observed occasional seizures in WT mice might be due to specific housing conditions or the paradigm used (presentation of two 2-min sounds [26]). Two consecutive injections 24 h apart significantly reduced the audiogenic seizure susceptibility in male and female *Fmr1*^{KO} mice tested 1 h after the second injection (Fig. 2e). Again, similar trends were observed using the scoring scale (Fig. S4d), and no sex-dependent differences were detected (Fig. S4e).

P110β inhibition normalizes altered open field and marble burying behavior in *Fmr1*^{KO} mice

We next tested the effect of pharmacological p110β inhibition on several behavioral and cognitive assays used in mouse models of FXS. In all assays, except nesting (Fig. 4b–d; Fig. S6f) and an operant conditioning task (Fig. 5; Fig. S7), mice received one injection of drug or vehicle 1 h before the experiment. Several assays were performed on the same cohorts of mice, but the experiments and thus drug injections were in all cases at least 5 days apart, a time when we assume the drug effect has completely vanished (see Fig. S2e, f). A detailed timeline of the assays, drug dosing, and age of the mice for each experimental group are shown in Fig. S5.

First, we assessed whether GSK6A affects altered open field behavior in *Fmr1*^{KO} mice. *Fmr1*^{KO} mice spent significantly more time in the center zone of the arena and entered the center zone more frequently compared to WT mice (Fig. 3a, b). One hour after GSK6A injection, *Fmr1*^{KO} mice spent less time in the center, entered the center less frequently, and were indistinguishable

from vehicle-treated WT mice (Fig. 3a, b). GSK6A-treated or vehicle-treated *Fmr1*^{KO} mice and WT mice did not differ in the distance traveled, suggesting the absence of overall locomotor effects of drug or genotype in an open field (Fig. 3c). FXS mice show increased marble burying and enhanced self-grooming [36]. One injection of GSK6A normalized excessive marble burying to WT levels in *Fmr1*^{KO} mice, but had no significant effect on this behavior in WT littermates (Fig. 3d). We next tested the effect of GSK6A on time spent grooming. Although there was a significant drug–genotype interaction, and, on average, *Fmr1*^{KO} mice appeared to spend more time grooming than WT mice, which was reduced with GSK6A, we did not detect significant differences in pairwise comparisons (Fig. S6a).

P110β inhibition restores social interaction in *Fmr1*^{KO} mice

To assess the effect of GSK6A on impaired sociability in *Fmr1*^{KO} mice, we next used a three-chamber social interaction test, in which mice were allowed to interact with an unfamiliar mouse in one chamber or an object in another chamber. Mice were injected with GSK6A or vehicle 1 h before testing. Vehicle-treated WT mice spent significantly more time in the chamber with the mouse than with the object. In contrast, vehicle-treated *Fmr1*^{KO} mice showed no preference (Fig. 4a). After GSK6A treatment, *Fmr1*^{KO} mice spent more time in the chamber with the mouse, suggesting increased sociability. GSK6A treatment in WT mice blunted social preference, which corroborates a role for p110β in social behavior (further discussed below). Very similar results were obtained when time spent close to the enclosure was analyzed (3 cm radial distance; Fig. S6b), and no significant group differences in chamber entries were detected (Fig. S6c). GSK6A slightly reduced mean distance traveled and mean speed regardless of genotype (Fig. S6d, e).

Fmr1^{KO} mice are worse nest builders than their WT littermates, creating aberrant, disorganized nests [37]. One single or two consecutive daily injections of GSK6A did not significantly alter nest building in WT or *Fmr1*^{KO} mice (Fig. 4b–d; Fig. S6f).

P110β inhibition rescues decision-making abnormalities in *Fmr1*^{KO} mice

To evaluate the potential of pharmacological inhibition of p110β to improve higher-order cognition in FXS, we next tested how GSK6A affects decision making. We have shown previously that *Fmr1*^{KO} mice and mice with prefrontal cortex-selective *Fmr1* knockdown (PFC-*Fmr1*^{KD}) are impaired in an operant conditioning assay [20]. As in our previous study, we generated PFC-*Fmr1*^{KD} mice by stereotaxic injection of *Fmr1* short hairpin RNA (shRNA)-expressing lentivirus into the prefrontal cortex (see Supplementary Material and Methods for details). Knockdown of FMRP was confirmed using tissue punches extracted from the prefrontal cortex (Fig. 5a). An overview of the testing and training paradigm is shown in Fig. 5b (also see Supplementary Material and Methods). Briefly, mice were trained to associate nose pokes at two different apertures with food reward. Then, the action–outcome association for one aperture was "degraded" (mice received food, uncoupled from nose pokes), whereas the other response remained rewarded (no change). Mice were then tested for their response preference. Next, the response contingencies were reversed, and response preferences were tested again. We replicated our previous results, showing that PFC-

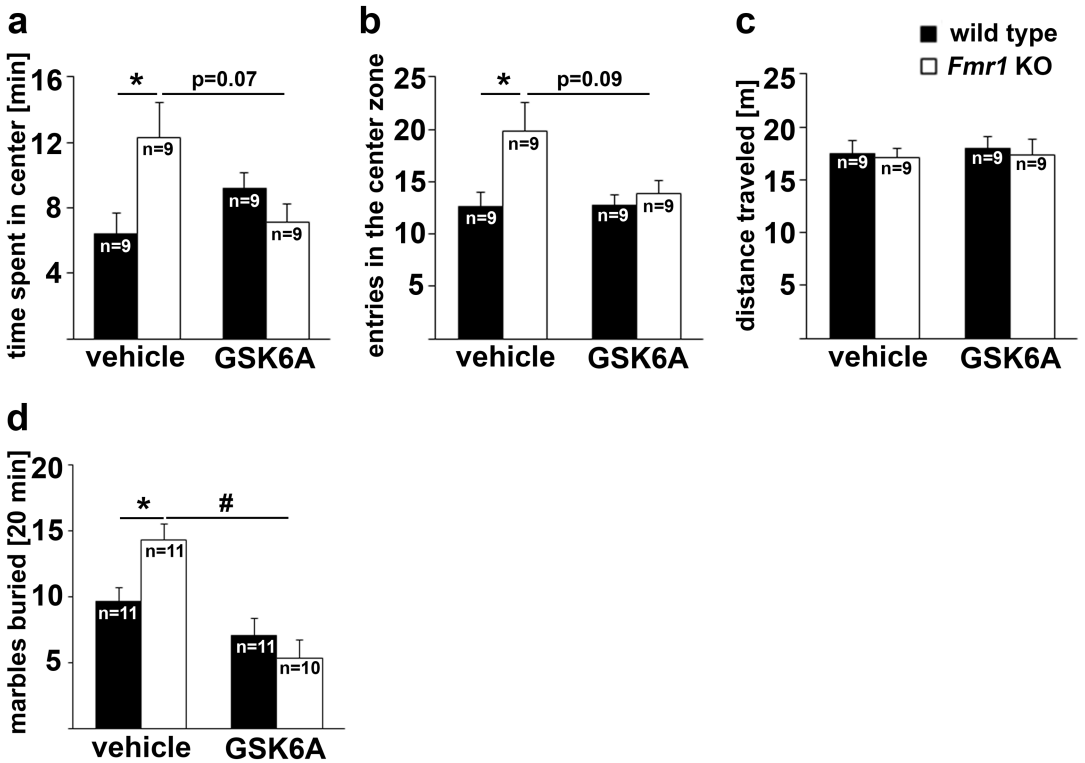

Fig. 3 GSK6A corrects open field behavior and marble burying in *Fmr1*^{KO} mice. **a**–**c** GSK6A normalized excess time spent in the center of an open field arena (**a**: two-way ANOVA with Tukey's post hoc tests: p(drug) = 0.419, F(1,32) = 0.7; p(genotype) = 0.191, F(1,32) = 1.8; p(interaction) = 0.009, F(1,32) = 7.7; *p = 0.031, p(ko/veh-ko/6 A) = 0.07), as well as increased frequency to enter the center (**b**: two-way ANOVA with Tukey's post hoc tests: p(drug) = 0.102, F(1,32) = 2.8; p(genotype) = 0.023, F(1,32) = 5.7; p(interaction) = 0.09, F(1,32) = 3.1; *p = 0.03, p(ko/veh-ko/6 A) = 0.09). The distance traveled in the open field arena did not differ between the groups (**c**: two-way ANOVA: p(drug) = 0.74, F(1,32) = 0.1; p(genotype) = 0.64, F(1,32) = 0.2; p(interaction) = 0.94, F(1,32) = 0.01). **d** GSK6A treatment reduced excessive marble burying in *Fmr1*^{KO} mice to WT levels (two-way ANOVA, Tukey's post hoc tests: p(drug) < 0.0001, F(1,39) = 20.8; p(genotype) = 0.230, F(1,39) = 1.5; p(interaction) = 0.011, F(1,39) = 7.1; *p = 0.040, $^{\#}p$ < 0.0001)

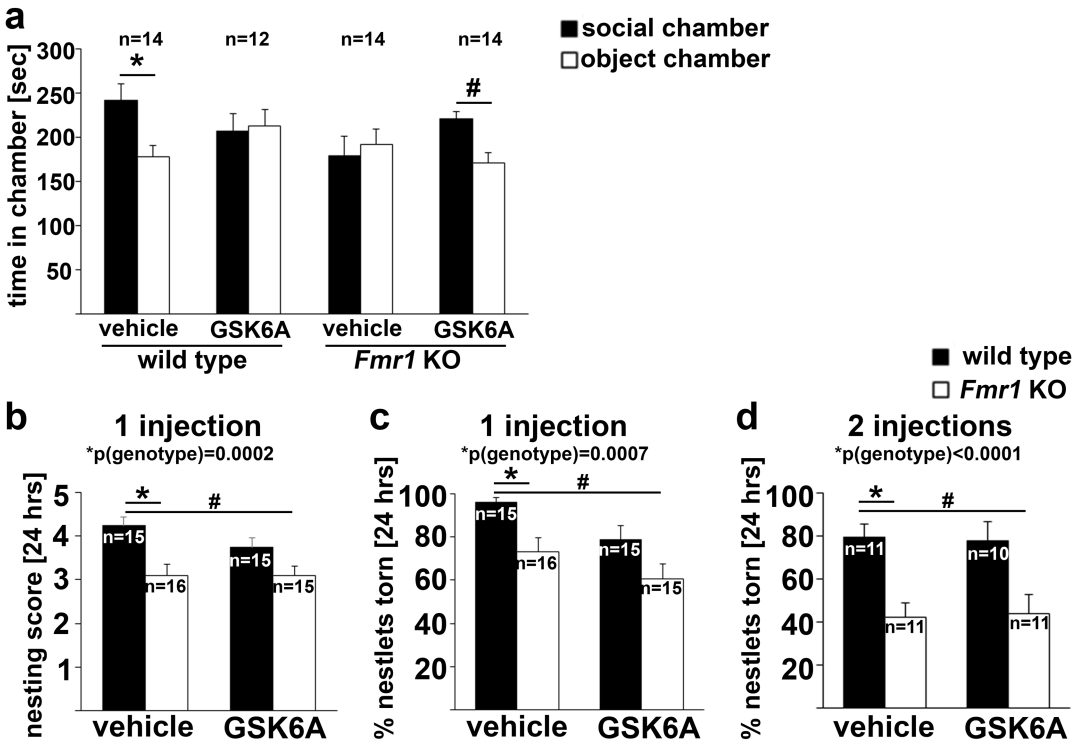

Fig. 4 Impaired social interactions, though not nest building in *Fmr1*^{KO} mice are improved by GSK6A. **a** In a three-chamber social interaction assay, vehicle-treated WT mice spent more time in a chamber associated with a conspecific than an object, whereas vehicle-treated *Fmr1*^{KO} mice did not show a preference. In contrast, GSK6A-treated *Fmr1*^{KO} mice preferred the "social chamber" (three-way repeated-measures ANOVA: p(drug × genotype × chamber) = 0.018, F(1,50) = 6; $^{*}p = 0.037$, $^{\#}p = 0.008$). GSK6A treatment abolished social preference in WT mice. **b**–**d** Nest scores were lower (**b**) and percent torn nestlet was lower (**c**, **d**) in *Fmr1*^{KO} mice. One or two consecutive daily injection(s) of GSK6A were ineffective in improving nest scores (two-way ANOVAs with Tukey's post hoc tests: one injection (**b**): p(drug) = 0.28, F(1,57) = 1.2; p(genotype) = 0.0002, F(1,57) = 15.5; p(interaction) = 0.27, F(1,57) = 1.3; $^{*}p = 0.004$; $^{\#}p = 0.005$; p(ko/veh-ko/6A) > 0.999; two injections (data not shown): p(drug) = 0.59, F(1,39) = 0.3; p(genotype) < 0.0001, F(1,39) = 20.3; p(interaction) = 0.40, F(1,39) = 0.7; p(wt/veh-ko/veh) = 0.003; p(wt/veh-ko/6A) = 0.005; p(ko/veh-ko/6A) = 0.996) or improving percent nestlet torn (two-way ANOVAs with Tukey's post hoc tests; one injection (**c**): p(drug) = 0.014, F(1,57) = 6.5; p(genotype) = 0.0007, F(1,57) = 12.7; p(interaction) = 0.676, F(1,57) = 0.18; $^{*}p = 0.031$; $^{\#}p = 0.0004$; p(ko/veh-ko/6A) = 0.44; two injections (**d**): p(drug) = 0.99, F(1,39) = 0.0001; p(genotype) < 0.0001, F(1,39) = 20.8; p(interaction) = 0.82, F(1,39) = 0.1; $^{*}p = 0.008$; $^{\#}p = 0.012$; p(ko/veh-ko/6A) = 0.998). Representative images of nests are shown in Fig. S6f

Fmr1^{KD} mice were able to learn to nose poke and initially differentiate between responses that were more or less likely to be reinforced (Fig. S7a, b), but then failed to do so when the response–reward relationships were inverted (Fig. 5c). Administered immediately after the "degradation" training day (during memory consolidation), the p110β inhibitor restored behavioral flexibility, such that PFC-*Fmr1*^{KD} mice were able to selectively engage the response most likely to be reinforced (Fig. 5c). No defects in marble burying or nesting behavior were observed in the PFC-*Fmr1*^{KD} mice (Fig. S7c, d), confirming that behaviors that would not be expected to be affected by PFC function were indeed spared. Using gross tissue punches extracted from the prefrontal cortex, we also found that site-selective *Fmr1* knockdown increased phosphorylation of Akt, which was normalized to control levels by GSK6A treatment 1 h before tissue collection (Fig. 5d).

The decision-making profiles described above can also be expressed as preference ratios wherein ratios >1 indicate a preference for the reinforced (rewarded) response, whereas a ratio of 1 reflects non-selective responding (i.e., a cognitive impairment). As expected, vehicle-treated PFC-*Fmr1*^{KD} mice generated a ratio of 1, and we detected a robust main effect of GSK6A (ratio >1), suggesting that in both control and *Fmr1* knockdown mice, p110β inhibition improved goal-directed behavior and behavioral flexibility. Importantly, the same profile was detected in *Fmr1*^{KO} mice tested under identical conditions, suggesting that GSK6A likewise rescued behavioral flexibility in *Fmr1*^{KO} mice (Fig. 5e).

Last, *Fmr1*^{KO} and WT mice were trained to press a novel lever for a food reward. Then, we withheld the food pellets entirely to assess response extinction, a form of PFC-dependent learning and memory. We administered GSK6A immediately following an initial extinction training session, during the presumed consolidation of new learning. The next day, *Fmr1*^{KO} mice treated with vehicle generated more responding than other groups, indicating impaired extinction. GSK6A normalized responding, suggesting that extinction consolidation was rescued (Fig. 5f).

DISCUSSION

This study reveals that pharmacological inhibition of the PI3K catalytic isoform p110β rescues a broad-spectrum of phenotypes in an FXS mouse model. Our work therefore encourages future studies into the clinical efficacy of p110 isoform-selective inhibitors in individuals with FXS. From a more general perspective, this work demonstrates successful preclinical repurposing of a compound, which was originally developed to treat cancer, for a brain disorder.

FMRP associates with the mRNA of the PI3K catalytic subunit p110β and inhibits its translation, leading to increased levels and activity of p110β in FXS mouse models and cells from individuals with FXS [16–19, 38]. Here we show that GSK6A, a p110β isoform-selective inhibitor, reduced aberrant molecular signaling, protein synthesis, dendritic spine density, and hippocampal LTD, reversed behavioral abnormalities and improved cognitive

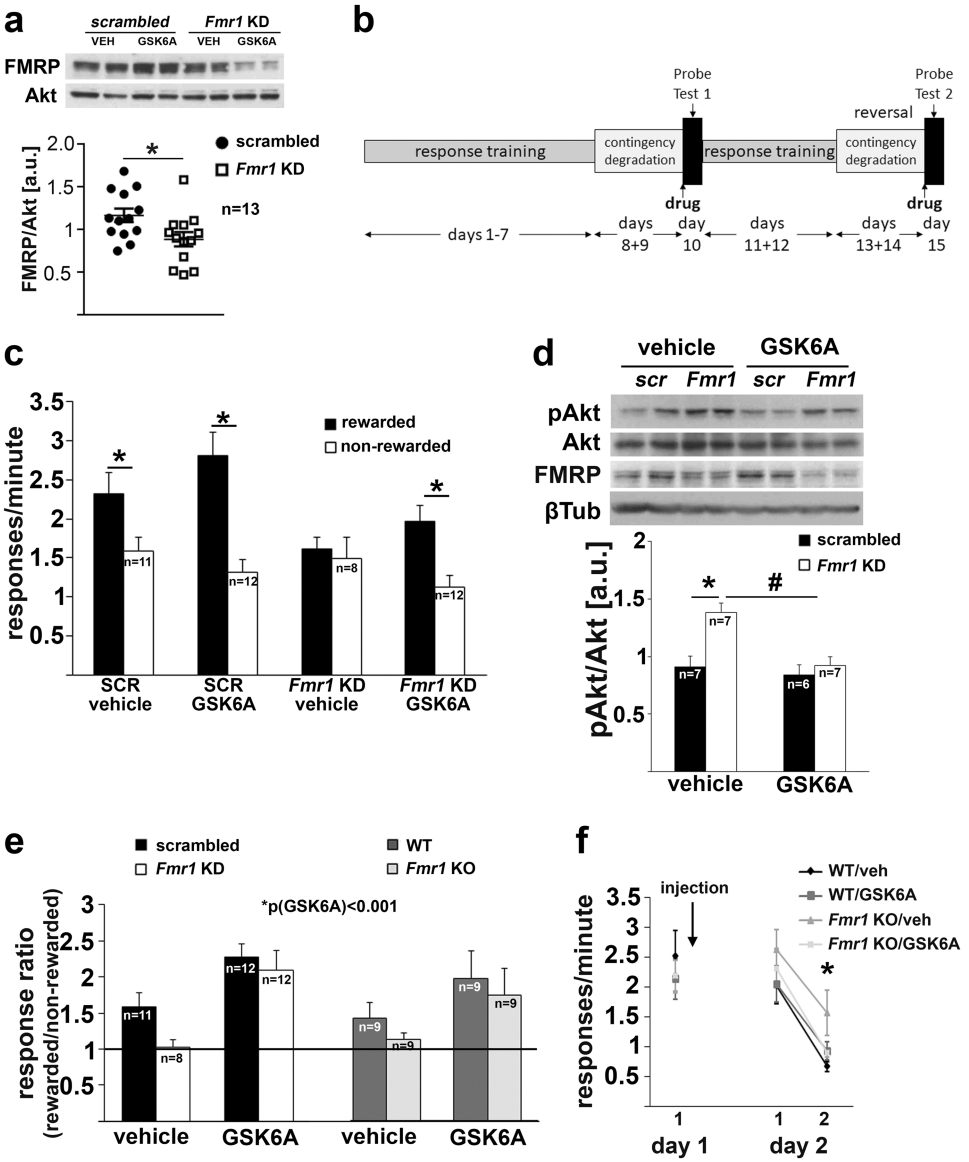

Fig. 5 Impaired decision making in PFC-*Fmr1*^{KD} mice and in Fmr1^{KO} mice is normalized by pharmacological inhibition of p110β. **a** FMRP is reduced in gross prefrontal cortical tissue punches containing both infected and non-infected tissue from mice injected with *Fmr1* shRNA-expressing lentivirus compared to scrambled shRNA-expressing lentivirus ($n = 13$, independent t test, $t(24) = 2.431$, $^{*}p = 0.023$). Representative western blot at top. Vehicle-treated and drug-treated mice were combined for the analysis. **b** Timeline of the PFC-dependent reward-related decision-making task to test goal-directed behavior in FMRP-deficient mice. (Note that *Fmr1*^{KO} mice were additionally tested in an extinction assay following this test.) **c** PFC-selective *Fmr1* knockdown mice initially learn to differentiate between rewarded and non-rewarded actions (Fig. S7a, b). However, after reversal of the response–reward contingencies, they respond non-selectively. GSK6A rescued these deficits (three-way ANOVA, p(Fmr1 × GSK6A × response choice interaction) = 0.036, F(1,40) = 4.7; post hoc $^{*}p < 0.05$). **d** Western blot analyses of PFC tissue punches confirmed that site-selective *Fmr1* knockdown increased Akt phosphorylation, which was normalized to WT levels with GSK6A (two-way ANOVA with Tukey's post hoc tests: p(drug) = 0.0043, F(1,23) = 10.0; p(shRNA) = 0.0032, F(1,23) = 10.8; p(interaction) = 0.032, F(1,23) = 5.2; $^{*}p = 0.0028$, $^{\#}p = 0.0035$). **e** Ratios of rewarded/non-rewarded responses showed lack of discrimination (ratio of 1) in both PFC-selective *Fmr1* knockdown mice (black/white) and constitutive *Fmr1*^{KO} mice (dark gray/light gray), which was rescued by GSK6A treatment in both conditions (both, two-way ANOVA: p(drug) < 0.001; F(1,72) = 17.2). **f** *Fmr1*^{KO} mice also show impaired response extinction, which was normalized to control levels by GSK6A (three-way repeated-measures ANOVA, p(genotype × treatment × session) = 0.042, F(2,62) = 3.33; post hoc $^{*}p < 0.05$)

function in FXS mice. This broad-spectrum phenotypic rescue spanning molecular, cellular, behavioral, and cognitive domains, together with previous findings that p110β is directly regulated by FMRP, supports our hypothesis that GSK6A targets a disease mechanism contributing to FXS etiology. Further supporting this notion, GSK6A had a significantly stronger effect on Akt phosphorylation in *Fmr1*^{KO} hippocampal slices compared to WT (Fig. 1e). P110β-selective inhibition also reduced elevated protein synthesis in *Fmr1*^{KO} hippocampus but did not affect protein synthesis rates in WT conditions (Fig. 1f). This suggests that overactive p110β is a critical mediator of aberrant PI3K signaling and protein synthesis in the hippocampus of *Fmr1*^{KO} mice.

Previous studies have shown increased S6 phosphorylation in *Fmr1*^{KO} mice, and genetic or pharmacologic reduction of S6 kinase, a direct regulator of S6, rescued molecular, cellular, and behavioral phenotypes in *Fmr1*^{KO} mice [12, 24]. Here, we did not

detect a genotype-dependent or drug-dependent difference in S6 phosphorylation (Fig. S3). S6 phosphorylation is sensitive to environmental factors such as novelty and age [32]. We thus speculate that the sound exposure (Fig. S3a–f), housing conditions (Fig. S3g–i), or age might have masked a potential increase in S6 phosphorylation in *Fmr1*^{KO} mice in our study. Nevertheless, we report a robust effect of drug and genotype on Akt phosphorylation, a more immediate downstream target of PI3K activity (Figs. 1c–e, 5d; Fig. S2).

In line with the reduction of enhanced protein synthesis and signal transduction, GSK6A also normalized exaggerated mGlu1/5-dependent LTD in *Fmr1*^{KO} hippocampal slices (Fig. 2b, c). The exact mechanisms of how p110β inhibition rescues the LTD phenotype in FXS are unclear. Previous studies have shown that dysregulated expression of specific proteins, such as Arc/Arg3.1 or CaMK2α, plays a role in exaggerated LTD in FXS [39, 40]. Correction of Arc/Arg3.1 and CaMK2α expression through GSK6A's effect on overall protein synthesis might thus partly contribute to the observed rescue of altered LTD. Increased CaMK2α leads to enhanced phosphorylation of the scaffolding protein Homer, which impairs its coupling to mGlu1/5 receptors [40], a mechanism suggested to underlie the LTD phenotype in FXS [41]. Of note, in addition to CaMK2α, Homer appears to be phosphorylated by Akt [42]. It will be interesting to test whether reduction of overactive Akt in *Fmr1*^{KO} hippocampal slices by p110β inhibition reduces phosphorylation of Homer and thus contributes to the rescue of exaggerated LTD.

GSK6A normalized behavioral impairments in FXS mice in a wide range of paradigms at the same dose that normalized increased PI3K signaling in hippocampus, cortex, amygdala, nucleus accumbens, and paraventricular nucleus of the thalamus. We speculate that this correction of signal transduction may transiently restore normal synaptic plasticity in these brain areas, thereby improving a variety of behavioral functions. A limitation of this study was that, except for the assessment of dendritic spine density, we only tested the effect of acute GSK6A administration. Notably, impaired nesting behavior was not rescued with one or two injections of GSK6A (Fig. 4b–d), and audiogenic seizures were only reduced after two consecutive doses (Fig. 2d, e). Chronic drug dosing may thus be necessary to rescue certain behaviors.

Daily treatment with the drug for 10 days (to assess effects on dendritic spine density, Fig. 2a) had no obvious effect on overall health of the mice. Mammals express four different isoforms of the class 1 PI3K catalytic subunit, which have overlapping and unique functions [43]. We speculate that these other PI3K isoforms can compensate for chronically reduced p110β activity to sustain essential non-neuronal functions of PI3K signaling, such as cell growth and proliferation. GSK6A reduced distance traveled in the social paradigm regardless of genotype, in contrast to our results in the open field paradigm. A previous study showed that chronic treatment with different PI3K isoform-selective inhibitors at high doses for several weeks reduced activity in mice during the light phase [44]. However, one dose of a selective inhibitor to p110δ did not affect basal locomotor activity in mice [45], in line with our results. We therefore conclude that the effect in the social interaction assay was paradigm-related and not due to overall reduction in activity.

In some instances, we observed an effect of GSK6A on behavior in WT mice, in addition to the rescue of phenotypes in *Fmr1*^{KO} mice. Several other p110 isoforms were reported to influence cognition and behavior in mice, with sometimes opposing effects of what we have observed with p110β inhibition. Genetic deletion of the class 1b PI3K subunit p110γ, for example, reduced behavioral flexibility [46]. In contrast, p110β inhibition overall improved behavioral flexibility in *Fmr1*-intact control mice in our study (Fig. 5c, e). Moreover, the p110β inhibitor blunted the preference of WT mice for another mouse vs. an object in the social interaction assay (Fig. 4a), whereas an inhibitor of the closely related class 1a PI3K isoform p110δ did not affect WT mice in a similar social interaction paradigm, but rescued impaired social interaction and cognition in a mouse model of schizophrenia [47]. As correction of excess p110β activity in *Fmr1*^{KO} mice rescued a deficit in social behavior, we hypothesize that tightly regulated p110β activity is essential for typical social behavior. Together, these studies demonstrate important and selective functions of p110 isoforms in behavior and cognition.

Several other behaviors, such as audiogenic seizures, nesting, and open field behavior, appeared to be changed by the p110β inhibitor in WT, although none of those effects reached significance. Nevertheless, the fact that GSK6A alters behavior in WT mice supports the argument that finely regulated p110β activity is essential for normal behavior. Chronic treatment studies with therapeutically relevant doses in *Fmr1*^{KO} mice are needed to assess whether p110β inhibition has undesirable side effects, in addition to its favorable effects on molecular, cellular, behavioral, and cognitive phenotypes.

FXS is by far not the only brain disorder characterized by altered signaling through the PI3K/mTOR pathway [2, 48, 49]. While the PI3K/mTOR pathway is pharmacologically targetable, its general inhibition can have severe side effects. Strategies that use PI3K isoform-selective inhibitors that only partially inhibit the PI3K/mTOR pathway, as done in this study, could thus be beneficial for many brain disorders.

GSK6A is a closely related analog to a compound that was originally developed for cancer treatment and is currently being evaluated in clinical trials with cancer patients. Our preclinical study in mice suggests that p110β-selective inhibitors, such as GSK6A, may improve phenotypes in FXS, and could thus be repositioned for the use in this brain disorder. This is in line with recent observations that the same pathways are often affected in cancer and autism [50]. Common mechanisms for altered cell growth control and synapse function due to overactive PI3K support the idea that selective inhibitors that were developed for the treatment of cancer may prove useful for autism. By exploring these shared pathways, translational research in FXS could greatly benefit from the advances in drug development for cancer treatment.

ACKNOWLEDGEMENTS

We thank Jeffrey Rymer, Nathan Petts, Joun Y. Lee, and Jingsheng Gu for technical assistance, and Emanuela Santini as well as all members of the Bassell, Gourley, and Gross labs for helpful discussions. This research was funded by NIH grants R21MH103748 (to C.G., S.L.G.) and 1U54HD082013 (to G.J.B.), a NARSAD Independent Investigator Award from the Brain and Behavior Research Foundation (to C.G.), two Summer Student Fellowships from the National Fragile X Foundation (to J.C.K., N.A.E.), the Cincinnati Children's Research Foundation (to C.G.), and Children's Healthcare of Atlanta (to S.L.G.). The Yerkes National Primate Research Center is supported by the Office of Research Infrastructure Programs/OD P51OD011132.

ADDITIONAL INFORMATION

Supplementary Information accompanies this paper at (https://doi.org/10.1038/s41386-018-0150-5).

Competing interests: GSK6A was obtained through a Material Transfer Agreement from GlaxoSmithKline. R.A.R. is an employee of GlaxoSmithKline, who owns GSK6A, and is co-inventor on US patents US 20130157977A1 and US 8778937B2. C.G. and G.J.B. are co-inventors on provisional patent application 62/680,050. All other authors declare no competing interests.

REFERENCES

1. Crino PB. The mTOR signalling cascade: paving new roads to cure neurological disease. Nat Rev Neurol. 2016;12:379–92.
2. Lipton Jonathan O, Sahin M. The neurology of mTOR. Neuron. 2014;84:275–91.

3. Gross C, Hoffmann A, Bassell GJ, Berry-Kravis EM. Therapeutic strategies in fragile X syndrome: from bench to bedside and back. Neurotherapeutics. 2015;12:584–608.
4. Richter JD, Bassell GJ, Klann E. Dysregulation and restoration of translational homeostasis in fragile X syndrome. Nat Rev Neurosci. 2015;16:595–605.
5. Qin M, Kang J, Smith CB. Increased rates of cerebral glucose metabolism in a mouse model of fragile X mental retardation. Proc Natl Acad Sci USA. 2002;99:15758–63.
6. Weiler IJ, Spangler CC, Klintsova AY, Grossman AW, Kim SH, Bertaina-Anglade V, et al. Fragile X mental retardation protein is necessary for neurotransmitter-activated protein translation at synapses. Proc Natl Acad Sci USA. 2004;101:17504–9.
7. Muddashetty RS, Kelic S, Gross C, Xu M, Bassell GJ. Dysregulated metabotropic glutamate receptor-dependent translation of AMPA receptor and postsynaptic density-95 mRNAs at synapses in a mouse model of fragile X syndrome. J Neurosci. 2007;27:5338–48.
8. Huber KM, Gallagher SM, Warren ST, Bear MF. Altered synaptic plasticity in a mouse model of Fragile X mental retardation. Proc Natl Acad Sci USA. 2002;99:7746–50.
9. Bear MF, Huber KM, Warren ST. The mGluR theory of Fragile X mental retardation. Trends Neurosci. 2004;27:370–7.
10. Scharf SH, Jaeschke G, Wettstein JG, Lindemann L. Metabotropic glutamate receptor 5 as drug target for Fragile X syndrome. Curr Opin Pharmacol. 2015;20C:124–34.
11. Berry-Kravis E, Des Portes V, Hagerman R, Jacquemont S, Charles P, Visootsak J, et al. Mavoglurant in Fragile X syndrome: results of two randomized, double-blind, placebo-controlled trials. Sci Transl Med. 2016;8:321ra325–321ra325.
12. Bhattacharya A, Mamcarz M, Mullins C, Choudhury A, Boyle RG, Smith DG, et al. Targeting translation control with p70 S6 kinase 1 inhibitors to reverse phenotypes in Fragile X syndrome mice. Neuropsychopharmacology. 2016;41:1991–2000.
13. Gantois I, Khoutorsky A, Popic J, Aguilar-Valles A, Freemantle E, Cao R, et al. Metformin ameliorates core deficits in a mouse model of fragile X syndrome. Nat Med. 2017;23:674–7.
14. Brown V, Jin P, Ceman S, Darnell JC, O'Donnell WT, Tenenbaum SA, et al. Microarray identification of FMRP-associated brain mRNAs and altered mRNA translational profiles in fragile X syndrome. Cell. 2001;107:477–87.
15. Darnell JC, Van Driesche SJ, Zhang C, Hung KY, Mele A, Fraser CE, et al. FMRP stalls ribosomal translocation on mRNAs linked to synaptic function and autism. Cell. 2011;146:247–61.
16. Ascano M Jr., Mukherjee N, Bandaru P, Miller JB, Nusbaum JD, Corcoran DL, et al. FMRP targets distinct mRNA sequence elements to regulate protein expression. Nature. 2012;492:382–6.
17. Miyashiro KY, Beckel-Mitchener A, Purk TP, Becker KG, Barret T, Liu L, et al. RNA cargoes associating with FMRP reveal deficits in cellular functioning in Fmr1 null mice. Neuron. 2003;37:417–31.
18. Gross C, Nakamoto M, Yao X, Chan CB, Yim SY, Ye K, et al. Excess phosphoinositide 3-kinase subunit synthesis and activity as a novel therapeutic target in fragile X syndrome. J Neurosci. 2010;30:10624–38.
19. Sharma A, Hoeffer CA, Takayasu Y, Miyawaki T, McBride SM, Klann E, et al. Dysregulation of mTOR signaling in Fragile X syndrome. J Neurosci. 2010;30:694–702.
20. Gross C, Raj N, Molinaro G, Allen AG, Whyte AJ, Gibson JR, et al. Selective role of the catalytic PI3K subunit p110beta in impaired higher order cognition in Fragile X syndrome. Cell Rep. 2015;11:681–8.
21. Dbouk HA, Backer JM. A beta version of life: p110β takes center stage. Oncotarget. 2010;1:729–33.
22. Li B, Sun A, Jiang W, Thrasher JB, Terranova P. PI-3 kinase p110β: a therapeutic target in advanced prostate cancers. Am J Clin Exp Urol. 2014;2:188–98.
23. Rivero RA, Tedesco R, Luengo JI. Benzimidazole boronic acid derivatives as PI3 kinase inhibitors. Google patents, 2014. https://www.google.com/patents/US8778937.
24. Bhattacharya A, Kaphzan H, Alvarez-Dieppa AC, Murphy JP, Pierre P, Klann E. Genetic removal of p70 S6 kinase 1 corrects molecular, synaptic, and behavioral phenotypes in fragile X syndrome mice. Neuron. 2012;76:325–37.
25. Deacon RM. Assessing nest building in mice. Nat Protoc. 2006;1:1117–9.
26. Thomas AM, Bui N, Graham D, Perkins JR, Yuva-Paylor LA, Paylor R. Genetic reduction of group 1 metabotropic glutamate receptors alters select behaviors in a mouse model for fragile X syndrome. Behav Brain Res. 2011;223:310–21.
27. Banerjee A, Luong JA, Ho A, Saib AO, Ploski JE. Overexpression of Homer1a in the basal and lateral amygdala impairs fear conditioning and induces an autism-like social impairment. Mol Autism. 2016;7:16.
28. Silverman JL, Yang M, Lord C, Crawley JN. Behavioural phenotyping assays for mouse models of autism. Nat Rev Neurosci. 2010;11:490–502.
29. Lin H, Erhard K, Hardwicke MA, Luengo JI, Mack JF, McSurdy-Freed J, et al. Synthesis and structure–activity relationships of imidazo[1,2-*a*]pyrimidin-5(1*H*)-ones as a novel series of beta isoform selective phosphatidylinositol 3-kinase inhibitors. Bioorg Med Chem Lett. 2012;22:2230–4.
30. Murakami H, Takanaga H, Matsuo H, Ohtani H, Sawada Y. Comparison of blood–brain barrier permeability in mice and rats using in situ brain perfusion technique. Am J Physiol Heart Circ Physiol. 2000;279:H1022–28.
31. Dwivedi Y, Rizavi HS, Teppen T, Zhang H, Mondal A, Roberts RC, et al. Lower phosphoinositide 3-kinase (PI 3-kinase) activity and differential expression levels of selective catalytic and regulatory PI 3-kinase subunit isoforms in prefrontal cortex and hippocampus of suicide subjects. Neuropsychopharmacology. 2008;33:2324–40.
32. Biever A, Valjent E, Puighermanal E. Ribosomal protein S6 phosphorylation in the nervous system: from regulation to function. Front Mol Neurosci. 2015;8:75.
33. Pende M, Um SH, Mieulet V, Sticker M, Goss VL, Mestan J, et al. S6K1(−/−)/S6K2(−/−) mice exhibit perinatal lethality and rapamycin-sensitive 5′-terminal oligopyrimidine mRNA translation and reveal a mitogen-activated protein kinase-dependent S6 kinase pathway. Mol Cell Biol. 2004;24:3112–24.
34. Schmidt EK, Clavarino G, Ceppi M, Pierre P. SUnSET, a nonradioactive method to monitor protein synthesis. Nat Methods. 2009;6:275–7.
35. Yan QJ, Asafo-Adjei PK, Arnold HM, Brown RE, Bauchwitz RP. A phenotypic and molecular characterization of the fmr1-tm1Cgr fragile X mouse. Genes Brain Behav. 2004;3:337–59.
36. Kazdoba TM, Leach PT, Silverman JL, Crawley JN. Modeling fragile X syndrome in the Fmr1 knockout mouse. Intractable Rare Dis Res. 2014;3:118–33.
37. Udagawa T, Farny NG, Jakovcevski M, Kaphzan H, Alarcon JM, Anilkumar S, et al. Genetic and acute CPEB1 depletion ameliorate fragile X pathophysiology. Nat Med. 2013;19:1473–7.
38. Gross C, Bassell GJ. Excess protein synthesis in FXS patient lymphoblastoid cells can be rescued with a p110beta-selective inhibitor. Mol Med. 2012;18:336–45.
39. Park S, Park JM, Kim S, Kim JA, Shepherd JD, Smith-Hicks CL, et al. Elongation factor 2 and fragile X mental retardation protein control the dynamic translation of Arc/Arg3.1 essential for mGluR-LTD. Neuron. 2008;59:70–83.
40. Guo W, Ceolin L, Collins KA, Perroy J, Huber KM. Elevated CaMKIIalpha and hyperphosphorylation of homer mediate circuit dysfunction in a fragile X syndrome mouse model. Cell Rep. 2015;13:2297–311.
41. Ronesi JA, Collins KA, Hays SA, Tsai NP, Guo W, Birnbaum SG, et al. Disrupted Homer scaffolds mediate abnormal mGluR5 function in a mouse model of fragile X syndrome. Nat Neurosci. 2012;15:431–40. S431
42. Huang GN, Huso DL, Bouyain S, Tu J, McCorkell KA, May MJ, et al. NFAT binding and regulation of T cell activation by the cytoplasmic scaffolding Homer proteins. Science. 2008;319:476–81.
43. Vanhaesebroeck B, Guillermet-Guibert J, Graupera M, Bilanges B. The emerging mechanisms of isoform-specific PI3K signalling. Nat Rev Mol Cell Biol. 2010;11:329–41.
44. Smith GC, Ong WK, Costa JL, Watson M, Cornish J, Grey A, et al. Extended treatment with selective phosphatidylinositol 3-kinase and mTOR inhibitors has effects on metabolism, growth, behaviour and bone strength. FEBS J. 2013;280:5337–49.
45. Law AJ, Wang Y, Sei Y, O'Donnell P, Piantadosi P, Papaleo F, et al. Neuregulin 1-ErbB4-PI3K signaling in schizophrenia and phosphoinositide 3-kinase-p110delta inhibition as a potential therapeutic strategy. Proc Natl Acad Sci USA. 2012;109:12165–70.
46. Kim JI, Lee HR, Sim SE, Baek J, Yu NK, Choi JH, et al. PI3Kgamma is required for NMDA receptor-dependent long-term depression and behavioral flexibility. Nat Neurosci. 2011;14:1447–54.
47. Papaleo F, Yang F, Paterson C, Palumbo S, Carr GV, Wang Y, et al. Behavioral, Neurophysiological, and synaptic impairment in a transgenic neuregulin1 (NRG1-IV) murine schizophrenia model. J Neurosci. 2016;36:4859–75.
48. Pilarski R, Burt R, Kohlman W, Pho L, Shannon KM, Swisher E. Cowden syndrome and the PTEN hamartoma tumor syndrome: systematic review and revised diagnostic criteria. J Natl Cancer Inst. 2013;105:1607–16.
49. Davis PE, Peters JM, Krueger DA, Sahin M. Tuberous sclerosis: a new frontier in targeted treatment of autism. Neurotherapeutics. 2015;12:572–83.
50. Crawley JN, Heyer W-D, LaSalle JM. Autism and cancer share risk genes, pathways, and drug targets. Trends Genet. 2016;32:139–46.